# AFRL-ML-WP-TP-2007-479

# PROTONATION AND CHEMICAL DOPING BEHAVIOR OF POLY(P-PHENYLENE BENZOBISTHIAZOLE) (BPZT): TOWARDS STABLE n-TYPE CONJUGATED POLYMERS (PREPRINT)

**Michael F. Durstock and Marc Mecoli**

**MARCH 2007**

STINFO COPY

**MATERIALS AND MANUFACTURING DIRECTORATE
AIR FORCE RESEARCH LABORATORY
AIR FORCE MATERIEL COMMAND
WRIGHT-PATTERSON AIR FORCE BASE, OH 45433-7750**

# NOTICE AND SIGNATURE PAGE

This report was cleared for public release by the Air Force Research Laboratory Wright Site (AFRL/WS) Public Affairs Office and is available to the general public, including foreign nationals. Copies may be obtained from the Defense Technical Information Center (DTIC) (http://www.dtic.mil).

AFRL-ML-WP-TP-2007-479 HAS BEEN REVIEWED AND IS APPROVED FOR PUBLICATION IN ACCORDANCE WITH ASSIGNED DISTRIBUTION STATEMENT.

*//Signature//                                                  //Signature//

MICHAEL F. DURSTOCK, Project Engineer        JOHN F. MAGUIRE, Chief
Polymer Branch                                              Polymer Branch
Nonmetallic Materials Division                        Nonmetallic Materials Division

//Signature//

SHASHI K. SHARMA, Acting Deputy Chief
Nonmetallic Materials Division
Materials and Manufacturing Directorate

This report is published in the interest of scientific and technical information exchange, and its publication does not constitute the Government's approval or disapproval of its ideas or findings.

*Disseminated copies will show "//Signature//" stamped or typed above the signature blocks.

# REPORT DOCUMENTATION PAGE

*Form Approved*
*OMB No. 0704-0188*

| 1. REPORT DATE *(DD-MM-YY)* | 2. REPORT TYPE | 3. DATES COVERED *(From - To)* |
|---|---|---|
| March 2007 | Journal Article Preprint | N/A |

**4. TITLE AND SUBTITLE**

PROTONATION AND CHEMICAL DOPING BEHAVIOR OF POLY(P-PHENYLENE BENZOBISTHIAZOLE) (BPZT): TOWARDS STABLE n-TYPE CONJUGATED POLYMERS (PREPRINT)

**5a. CONTRACT NUMBER**
In-house

**5b. GRANT NUMBER**

**5c. PROGRAM ELEMENT NUMBER**
62102F

**6. AUTHOR(S)**

Michael F. Durstock and Marc Mecoli

**5d. PROJECT NUMBER**
4347

**5e. TASK NUMBER**
RG

**5f. WORK UNIT NUMBER**
M01R1000

**7. PERFORMING ORGANIZATION NAME(S) AND ADDRESS(ES)**

Polymer Branch (AFRL/MLBP)
Nonmetallic Materials Division
Materials and Manufacturing Directorate
Air Force Research Laboratory, Air Force Materiel Command
Wright-Patterson Air Force Base, OH 45433-7750

**8. PERFORMING ORGANIZATION REPORT NUMBER**

AFRL-ML-WP-TP-2007-479

**9. SPONSORING/MONITORING AGENCY NAME(S) AND ADDRESS(ES)**

Materials and Manufacturing Directorate
Air Force Research Laboratory
Air Force Materiel Command
Wright-Patterson AFB, OH 45433-7750

**10. SPONSORING/MONITORING AGENCY ACRONYM(S)**
AFRL/MLBP

**11. SPONSORING/MONITORING AGENCY REPORT NUMBER(S)**
AFRL-ML-WP-TP-2007-479

**12. DISTRIBUTION/AVAILABILITY STATEMENT**

Approved for public release; distribution unlimited.

**13. SUPPLEMENTARY NOTES**

Journal article submitted to the Journal of the American Chemical Society. This is a work of the U.S. Government and is not subject to copyright protection in the United States.

PAO Case Number: AFRL/WS 07-0792, 03 Apr 2007. This paper contains color content.

**14. ABSTRACT**

Poly(p-phenylene benzobisthiazole) (PBZT) is a rigid-rod polymer that has been thoroughly studies for its good mechanical and thermo-oxidative properties. Recently, however, it was discovered that PBZT also exhibits quite interesting and unusual optical and electrical properties that are highly dependent upon the presence of an acid within the film, which acts to protonate the nitrogen sites in the aromatic heterocycle. When protonated, this material becomes a very good electron acceptor and can be n-type (reductively) doped with a variety of metals to yield a high conductive material. The doped material is stable with respect to water, but becomes de-doped in the presence of oxygen. A thorough examination of the protonation and chemical doping behavior of thin films of PBZT in a variety of different acids is presented and a general mechanism is discussed.

**15. SUBJECT TERMS**

n-doping, conjugated polymer, PBZT

**16. SECURITY CLASSIFICATION OF:**

| a. REPORT | b. ABSTRACT | c. THIS PAGE |
|---|---|---|
| Unclassified | Unclassified | Unclassified |

**17. LIMITATION OF ABSTRACT:** SAR

**18. NUMBER OF PAGES** 38

**19a. NAME OF RESPONSIBLE PERSON** (Monitor)
Michael F. Durstock

**19b. TELEPHONE NUMBER** *(Include Area Code)*
N/A

**Standard Form 298 (Rev. 8-98)**
Prescribed by ANSI Std. Z39-18

**Introduction**

Conjugated polymers have been studied in great detail over the past several decades due to their unique optical and electronic properties and the potential to use them in a variety of active devices including LEDs, photovoltaics, electrochromics, transistors, and others. Virtually all of the device applications that have been studied to date rely on the conjugated polymer being in either the chemically undoped state or being p-type (oxidatively) doped. There are many applications that would benefit tremendously from the availability of n-type (reductively) doped materials, however most of those systems studied are quite unstable towards re-oxidation in the ambient environment. Towards this goal, a variety of groups have been focused on designing and synthesizing new n-type doped conjugated polymer systems,[1-34] however no environmentally stable system has been achieved.

One particularly interesting and relevant material is the rigid-rod polymer poly(p-phenylene benzobisthiazole) (PBZT). This material, along with the related benzobisoxazole and benzobisimidazole analogues, has been studied in depth for its good mechanical and thermo-oxidative properties which are particularly beneficial for structural applications.[35] Recently, however, it was discovered that PBZT also exhibits quite interesting and unusual optical and electrical properties that are highly dependent upon the presence an acid within the film which acts to protonate the nitrogen sites in the aromatic heterocycle.[7-14] It is believed that this material, when protonated, becomes a very good electron acceptor and can be n-type (reductively) doped with a variety of metals to yield a highly conductive, relatively stable material.

1

It is the purpose of this paper to provide a thorough examination of both the protonation and chemical doping behavior of PBZT under a variety of different conditions. Four different acids are studied to examine the effects of the anion on the protonation and doping behavior and a variety of different metals are used to chemically dope the material, which is remarkably stable even when immersed in water. By examining this fundamental chemical and electronic behavior, we provide a more complete description of how this system behaves which can be generalized and applied to the further design of even more stable, n-type doped polymers.

**Experimental**

The glass slides that were used as substrates in these studies were first cleaned by sonicating them in a series of solutions. A mild detergent was followed by trichloroethane, acetone, and then methanol. In order to promote adhesion to the spin-coated films, the glass slides were modified by depositing an inert, thin polymer multilayer film using a layer-by-layer deposition approach.[36] Anywhere from 2 to 5 bilayers of a polycation (poly(allylamine hydrochloride)) and polyanion (polyacrylic acid or polystyrene sulfonate) combination were deposited onto the surface according to well established procedures.[36-39] Thin films of PBZT were spin-coated onto these substrates from a 0.1 weight percent solution in methanesulfonic acid. Typical spin-coating conditions were 500 rpm for 15 sec followed by 2000 rpm for 15 sec. The remaining acid was removed from the spin-coated film by soaking it in deionized water, which acted to coagulate the PBZT film and dissolve the methanesulfonic acid.

Absorption spectroscopy was performed on a Cary 5 UV-Vis-NIR spectrophotometer from Varian.  Spin-coated PBZT films were exposed to a variety of different aqueous, acidic solutions and the absorbance spectra were measured *in situ* according to the following procedure.  After spin coating the film, the glass slide was cut to fit into a 1 cm x 1 cm quartz cuvette, which was filled with the aqueous acid solution of interest.  A baseline scan was obtained prior to inserting the sample by using a blank substrate and the appropriate solution in the cuvette.  It should be noted that the absorbance for each of the various acid solutions are not the same due to the range of acid concentrations used.  Consequently, separate baselines were necessary for each scan in order to appropriately correct for the absorbance of the solution itself.

In the cases where a metal was in contact with the film and solution during the absorption measurement, a portion of the glass slide was first coated with a thin film of the appropriate metal.  This deposition was accomplished using a high-vacuum, thermal evaporation system at a base pressure of $10^{-6}$ torr or lower.  The PBZT film was subsequently spin-coated over the entire substrate, including the metallized portion.  During the absorption measurements, the metallized region was positioned in the acid solution and placed in close proximity to, but not overlapping with, the area over which the absorption was measured.

**Results and Discussion**

The serendipitous discovery that PBZT can become chemically doped and highly conductive when in the presence of an acid has been preliminarily reported on[7,8,13] and is shown in Figure 1.  PBZT (structure also shown in Figure 1) is an aromatic, heterocyclic,

rigid-rod polymer that is only soluble in strong acids. The acid acts to protonate the nitrogen sites in the heterocycle to disrupt the molecular packing and intermolecular interactions thereby enabling the polymer to be dissolved. A significant amount of work has gone into examining the lyotropic liquid crystalline behavior of these materials in solution[35], however it has only recently been discovered that a free-standing film of PBZT immersed in a more dilute acidic solution is capable of becoming doped and highly conductive. As shown in the figure, pristine PBZT forms a yellow film that remains unchanged when it is immersed in water. Upon immersion in concentrated hydrochloric acid, the polymer becomes protonated and turns orange in color. The startling observation is that if this protonated material is contacted by a piece of copper, the film turns very dark (black) in the area near the copper. This doped region grows radially out from the point of contact of the copper to encompass the entire film in a matter of seconds. The D.C. electrical conductivity of the doped film has been measured to be on the order of 100 S/cm, which is to be compared to approximately $10^{-12}$ S/cm for the pristine, undoped film.[7,8,13] This same effect has been observed spectroelectrochemically[8] whereby a film of PBZT is applied to a transparent electrode (Indium Tin Oxide) and used as the cathode in an electrochemical cell. The film becomes electrochemically reduced to give the same, doped form of PBZT as seen above. The prevailing thought on the mechanism of this process is that since protonation of the PBZT occurs at the N lone pair electrons ($\sigma$-system) which are orthogonal to the $\pi$-system, the effect on the $\pi$-orbitals is mainly to significantly increase the electron affinity and reduction potential of the polymer. A similar situation would result upon quaternization of the nitrogen with alkyl substituents and this has been a focus of the

work by Dudis and others[8,10,11,13]. It should be noted that Marks and coworkers first reported on the ability of PBZT to be electrochemically doped to yield an electrically conductive polymer.[40] That work focused on pristine PBZT that was not protonated and required $-1.47$ V vs SCE ($E_{1/2}$) in order to reduce to polymer.

As discussed in more detail later, the reduction potential is observed (via comparison to the standard reduction potentials of metals) to be significantly increased upon protonation with seeming little deleterious effect on the stability. In fact, if the doped material is subsequently removed from the concentrated HCl solution and put in de-ionized water under ambient conditions, the film remains in its doped state. Only after about 10 minutes does the film become de-doped and it returns to its original unprotonated and undoped form (yellow film). This process is completely reversible and the material will once again become protonated and doped if immersed into an acidic solution and contacted by a piece of copper. If the doped film is immersed in water that has been purged with $N_2$ gas to remove dissolved $O_2$, then the film remains in its doped state for about 45 minutes before becoming de-doped, and if the doping process is carried out in a $N_2$ purged glove bag, then the film remains doped for at least several days. Apparently, the doped form of PBZT is stable with respect to water, but is re-oxidized (i.e. unstable) in the presence of $O_2$.

To quantify the effects of protonation, UV-vis absorption spectroscopy was performed on thin films of PBZT exposed to different acidic conditions. Figure 2 shows the results for a spin-coated film of PBZT that is exposed to various concentrations of aqueous HCl solutions during the measurement. The spectrum for 0 M HCl (i.e. pure water) is that of pristine PBZT and exhibits two major peaks near 443 nm and 474 nm

which is consistent with what has been reported in the literature.[41-43] As the HCl concentration increases, the peaks at 443 nm and 474 nm decrease while a new peak at 499 nm grows, with an isosbestic point near 481 nm. At 12.1 M (concentrated solution, 37 wt%), the peak at 443 nm has effectively disappeared and the spectrum is again comprised of two major peaks, but now located at longer wavelengths. The presence of the isosbestic point strongly suggests that there are only two species contributing to the absorption spectrum over the concentration range studied. The first, which is characterized by the spectrum at 0 M, is that of the un-protonated form of PBZT. The second, which has the spectrum shown for 12.1 M, can reasonably be assumed to be the half-protonated form of PBZT in which only one of the N sites in the polymer repeat unit is protonated. The spectra shown for concentrations in between these two extremes are simply a linear combination of these two spectra which gives rise to the isosbestic point at 481 nm. This red-shift in the absorption spectrum upon protonation could be attributed to several factors. Shen and coworkers[41,42] have attributed a similar observation in model compounds to an increase in the electron delocalization between the main heterocyclic ring and the phenyl ring in the protonated structure, analogous to a longer conjugation length. However, a variety of other groups working on similar aromatic, N-containing heterocyclic polymers and compounds have seen very similar effects upon protonation and have attributed it to an electronic effect.[5-14,44-46] Protonation (and quaternization in general) of the N-lone pair electrons significantly lowers both the HOMO and LUMO levels by acting as an electron accepting substituent and introducing a positive charge onto the polymer. It lowers the LUMO more so than it does the HOMO, due to the greater electron density on the N-site in the LUMO, and therefore the optical gap is

decreased.[6,44] This explanation agrees with the chemical doping observations discussed later and is believed to be responsible for the shift seen here.

By plotting the peak absorbance values (at 443 nm, 474 nm, and 499 nm) for each of the different acid concentrations, spectrometric titration curves, such as that shown in Figure 2b can obtained.[47] As mentioned above, these measurements are performed on a thin film of PBZT that is in equilibrium with an aqueous, acidic solution. The acid concentrations range from 0 M (pure water) to concentrated stock solutions (37 wt% for HCl, 12.1 M). Since very concentrated solutions are being used (both here as well as in later discussions where the acid is close to 100 wt%), it is more appropriate to refer to the concentrations themselves rather than pH values, which would effectively become meaningless at the high concentrations discussed later. Consequently in order to determine "effective" $pK_a$ values of the PBZT films, the spectrometric titration curves are plotted using pHA values, whereby $pHA = -\log[HA]$ and [HA] is the concentration of the acid. In situations of low acid concentration, this is equivalent to the pH of the solution since the films used here are sufficiently thin so as to not appreciably affect the value.

The effective $pK_a$ for protonation of PBZT in HCl can be determined by the inflection point of all three curves in Figure 2b, and this occurs at a value of approximately $-0.8$. At this point, half of the polymer repeat units are mono-protonated and the other half are un-protonated. Protonation of the second nitrogen atom to give the fully protonated form would occur at higher acid concentrations than are achievable with aqueous hydrochloric acid (concentrated HCl $\sim$ 37 wt%), as discussed later.

This behavior is similar to other well-known, aromatic nitrogen-containing heterocyclic systems such as pyrazine and 4,4'-bipyridine in which protonation of the

7

two equivalent nitrogen atoms (lone pair electrons are similarly orthogonal to the $\pi$-system) occurs at separate $pK_a$ values.  The dissociation constants for the conjugate acid of pyrazine are $pK_{a1}$ = -6 ($PyzH_2^{2+}$) and $pK_{a2}$ = 0.6 ($PyzH^+$),[48] while for 4,4'-bipyridine they are $pK_{a1}$ = 2.5 ($BpyH_2^{2+}$) and $pK_{a2}$ = 4.9 ($BpyH^+$).[49]  It is useful to compare these values to that for pyridine itself which has a $pK_a$ = 5.2 ($PyH^+$).  From this comparison, the well-known electron-withdrawing effects of N are manifested by the fact that the $pK_a$ for mono-protonation follows the order $PyH^+$ > $BpyH^+$ > $PyzH^+$.  In addition, however, it can be seen that protonation of the first N-site results in a significant lowering of the basicity (lower $pK_a$) of the second N-site.  That is to say, $pK_{a2}$ > $pK_{a1}$ for both pyrazine and bipyridine.  In addition, based on infrared spectroscopic data of PBZT model compounds in solution, Shen and coworkers[41] have also concluded that the benzobisthiazole system exhibits two separate $pK_a$ values associated with each nitrogen atom.  However due to the fact that their studies were carried out on low-molecular weight compounds in a dilute solution, and those discussed here are for thin, solid films in equilibrium with an aqueous, acidic solution, significantly different results are obtained.  The results for the model compounds[41] yield an estimated $pK_a$ of 2.1 for mono-protonation which is to be compared to the value of $-$ 0.8 as discussed above.  Many factors could play a role in this discrepancy, however given that the thin film must maintain equilibrium with the aqueous solution, a partitioning of the acid between the two phases in accordance with the Nernst Distribution Law will likely occur.[50]  This would result in a lower effective pH in the film and could account for the observed difference as compared to the single-solution case for the model compounds.  If the simplifying assumption is made that the results for the model compound in solution are characteristic of the intrinsic protonation

behavior of benzobisthiazole, then an effective pH of 2.1 would be needed in the film to reach the equivalence point. Given that the pHCl (~pH) of the solution in equilibrium with the film at equivalence is observed to be −0.8, then a partition coefficient, $[HCl]_{aq}/[HCl]_{film}$, of about 800 can be estimated to exist between the aqueous, acidic solution and the thin film. While this large partitioning effect is consistent with the hydrophobic character of PBZT, other morphological or macromolecular effects could also account for some of the observed difference in the protonation behavior.

The same set of experiments as described for Figure 2 were performed on a thin film of PBZT that was in contact with a piece of copper when it was immersed in the aqueous, hydrochloric acid solution and the results are shown in Figure 3. Initially at low acid concentrations (0 to 6.0 M, pHCl > −0.8), the behavior is the same as that in the absence of the copper (Figure 2). That is, the absorbance peaks at 443 nm and 474 nm begin to decrease while that at 499 nm begins to grow with increasing acid concentration. However, once the pHCl of the aqueous solution reaches about −0.8, the film exhibits a completely different behavior which is characteristic of the black, doped film shown in Figure 1. The three individual peaks previously seen are no longer present, but rather a very broad and relatively featureless peak is observed which is typical of doped, conjugated polymers. This is shown in the spectrometric titration curve of Figure 3b by an increase in the absorbance peak intensity at 630 nm and a sharp decrease in the peak intensity at the other three wavelengths below a pHCl of −0.8. This transition occurs exactly at the $pK_a$ determined in Figure 2. Once the polymer becomes protonated (in this case, with a $Cl^-$ counter-ion), it is capable of being reduced by simple metals. Metallic copper donates an electron to the protonated PBZT, which results in $CuCl_2$ being formed

in the aqueous, acidic solution. Figure 4 supports this conclusion by showing the UV-vis absorption spectrum of the supernatant, HCl solution (baselined to concentrated HCl) after a film of PBZT has been doped with metallic copper. Clearly, $CuCl_2$ is present in the solution after the doping process. In addition, if a stoichiometric analysis is performed on the supernatant solution, the amount of $CuCl_2$ that is found in solution is $1.41 \times 10^{-5}$ mol for every 7.7 mg ($2.89 \times 10^{-5}$ mol) of polymer repeat units that have been doped. This corresponds to a molar ratio of 0.49 which indicates that there is a one-to-one correspondence between the number of polymer repeat units and the number of $Cl^-$ ions that get expelled into the solution during doping.

Cyclic voltammetry was performed in an attempt to precisely determine the reduction potential of the protonated polymer, however experimental complications made the results inconclusive. Poor adhesion of the films to the electrode surfaces, especially under acidic conditions, led to delamination. These efforts are continuing, however by generalizing the chemical doping process to include other metals, an indirect estimate of the reduction potential can be made. A film of PBZT immersed in concentrated HCl is able to be doped by a variety of metals including Mg, Al, Zn, Fe, Cu, and even Ag (but not Au), in a fashion similar to that described above. While exhaustive spectrometric titrations have not been performed for each of these metals, comparison to their standard electrode potentials results in the conclusion that the reduction potential of protonated PBZT is near 0.56 V vs SCE (standard electrode potential for $Ag^+ + e^- \rightarrow Ag$). Metals with an electrode potential lower than this are able to reduce the protonated PBZT. As mentioned above, Marks and coworkers[40] have measured the reduction potential for pristine PBZT and have shown it to be –1.47 V vs SCE. Consequently, protonation of

the N-site along the polymer backbone of PBZT results in a very large increase in the reduction potential (making it easier to reduce), which is responsible for the ability of the protonated polymer to be reduced by simple metals.

The proposed mechanism for protonation and chemical doping is shown in Figure 5. At relatively low acid concentrations (characteristic of protonation in HCl), the polymer becomes protonated at one of the N-sites in the repeat unit. This occurs at a characteristic $pK_a$ (–0.8 for HCl), as discussed in Figures 2 and 3 above. Once the polymer becomes protonated, it is capable of becoming reduced by simple metals to form the quinoidal structure shown in Figure 5d. It is useful to consider that the protonated form of PBZT can be classified as a Weitz-type redox system that is capable of a two-step, reversible reduction/oxidation.[51] This type of behavior is typified by the well-known class of materials known as 'viologenes' (N-alkylated 4,4'-bipyridines), as shown in Figure 6a.[51-53] Hünig proposed a general structural principle for these systems[51,54,55] in which the heteroatoms are members of a cyclic $\pi$-system showing "quinoid" behavior in the reduced form. Quaternization of both N-sites in 4,4'-bipyridine results in a system (OX state) that is iso-$\pi$-electronic with bi-phenyl, exhibits aromatic character, and is capable of a two-electron reduction that occurs in a step-wise fashion. Upon this two-electron reduction (RED state), the N-sites have a lone-pair of electrons that are part of the $\pi$-system, and it exhibits "quinoid" behavior due to the addition of these two electrons. The intermediate state (one-electron reduction, the so-called semiquinone (SEM) state) is the radical cation which can exhibit thermodynamic stability over the fully reduced state, depending upon the amount of separation between the two redox potentials, $E_1$ and $E_2$.

In addition to the viologens, this principle has successfully been applied to describe a great variety of other organic redox systems. These include the generic class of fulvalenes that is of such great interest in charge transfer salts, and many other related heterocyclic systems. As shown in Figure 5b and as pointed out by Bryce[56], the bis(benzothiazole)s can be viewed as extended analogues of tetrathiafulvalene (TTF) that exhibit Weitz-type behavior. Please note that in the figure, TTF and dibenzo-TTF are shown in their reduced form while bis(benzothiazole) is shown in the oxidized form. Inserting an aromatic group between the two heterocyclic rings simply acts to extend the π-system and thereby separate the positive charges depending on the size of the group. Bryce[56] found that in bis(benzothiazole) and related systems where a variety of extended, conjugated linking groups (phenyl, naphthyl, thiophene, etc.) were used instead of directly joining the two heterocyclic rings, the molecules undergo a single, reversible, two-electron reduction process to the RED state. This is in marked contrast to the more typical behavior of two, reversible, single-electron redox waves (first to the SEM and then to the RED state) as seen in the viologenes and TTF derivatives in which the rings are joined directly together and is a result of an increased separation (and less Coulombic repulsion) of the heterocyclic rings.

This two-electron redox behavior of bis(benzothiazole)s is in agreement with the doped form of PBZT shown in Figure 5d. The N-site on either side of the phenyl group is protonated and the polymer exhibits Weitz-type behavior by undergoing a two-electron reduction to give the quinoidal structure shown. The fact that a one-to-one correspondence is observed between the number of polymer repeat units and the number

12

of $Cl^-$ ions that get expelled into the solution during the doping process also supports the notion that the polymer is undergoing a two-electron reduction.

In order to probe the protonation and doping behavior of PBZT at even higher acid concentrations and with different anions, a variety of other acids were examined. Figure 5c shows the effect of exposing the PBZT film to even higher acid concentrations (concentrated sulfuric acid, 96 wt%, in this case). Qualitatively the film again turns yellow at these high concentrations, which is attributed to the second protonation step. Surprisingly, the film is unable to be chemically doped with simple metals in this fully protonated state. The UV-vis absorption and spectrometric titration data for a thin film of PBZT exposed to a range of $H_2SO_4$ concentrations is shown in Figure 7. Initially at low acid concentrations (0 to 9.0 M, $pH_2SO_4 > -0.95$), the film responds in the same manner as it did with HCl. The two peaks at 443 nm and 474 nm decrease while the one at 499 nm grows with an isosbestic point near 483 nm. The titration curve in Figure 7c also shows similar behavior over the $pH_2SO_4$ range from $-0.2$ to $-0.95$ with an inflection point corresponding to the $pK_a$ of the mono-protonated species located at about $-0.65$, although the spacing of the data makes a precise determination impossible. This value is close to that seen with HCl ($-0.8$), but the cause for the deviation is not completely understood. At higher $H_2SO_4$ concentrations (9.0 to 18.0 M, $pH_2SO_4 < -0.95$), completely different behavior is observed. Now as the acid concentration increases, the absorption spectrum moves back towards lower wavelengths (giving rise to the yellow color of the film again), but in a manner that is more consistent with the entire curve blue-shifting rather than the disappearance and emergence of two distinct spectra with an isosbestic point. This shift is likely the result of protonation of the second N-site on the PBZT, in which

case the $pK_a$ for this second protonation would be near –1.0 as shown in Figure 7c. The amount of shift is likely determined by a combination of electronic and ring torsion effects. Co-planarity between the phenyl and heterocyclic rings of PBZT will result in delocalization of the $\pi$ electrons. However as the rings become non-planar (i.e. a larger torsion angle, $\phi$), the effective conjugation length will decrease resulting in a blue-shifting of the absorption spectrum. Indeed, studies of PBZT have shown that it is non-planar.[57-62] Experimentally[57], the torsion angle of a model compound is measured to be near 23°, while theoretically[58] it is predicted to be 55°. The discrepancy is believed to be due to the significant impact that intermolecular interactions have on the chain conformation. A considerable rotational flexibility is predicted (low barrier to rotation), and when the intermolecular interactions are included in the model, much better agreement with experiment is achieved. Protonation of the PBZT chains greatly decreases these intermolecular interactions which is the reason that it is only soluble in strong acids.[59] Consequently at high levels of protonation, the torsion angle might be expected to increase due to a decrease in the intermolecular interactions, and thereby cause the observed blue-shift in the absorption spectrum. Similar effects have been observed in a variety of heterocyclic systems including poly(pyridine)[44,46] and bithiazole containing polymers.[5,6]

If the protonation in aqueous solutions of $H_2SO_4$ is carried out while the film of PBZT is in contact with a piece of metal, then the material can become chemically doped. Figure 8 shows the UV-vis absorption spectra and spectrometric titration data. As was the case for HCl, at low acid concentrations (0 to 5.4 M, $pH_2SO_4 > -0.7$) it behaves very much the same as in the absence of the metal. The absorbance peaks at 443 nm and 474

nm begin to decrease, while the peak at 499 nm grows with increasing acid concentration. At intermediate acid concentrations (7.2 M and 9.0 M), the material is in it's mono-protonated state and becomes doped as indicated by the very broad, long-wavelength absorption spectra. As before, this transition occurs very near the $pK_a$ determined for mono-protonation (–0.65) in Figure 7. However in this case, the doping was carried out by Fe because it is found that Cu will not induce doping at any level of protonation with $H_2SO_4$. Mg, Al, Zn and Fe (i.e. electrode potential at or below Fe), however, are all able to reduce the protonated PBZT at these intermediate acid concentrations. Consequently while the absorbance spectrum does not change significantly between HCl and $H_2SO_4$ and protonation by both acids yields a peak near 499 nm, the reduction potential does depend on the anion ($Cl^-$ or $HSO_4^-$) that is present. This is discussed in more detail below in comparison to other acids.

At high acid concentrations (Figure 8), PBZT is unable to be chemically doped by the Fe and the absorption spectrum reverts back to what it was in the absence of the metal. This transition occurs at the point (above 9.0 M, $pH_2SO_4 < -1.0$) where the blue-shifting in the absorption spectrum began in Figure 7 and which was attributed to the second protonation step of PBZT. The exact mechanism of this is unclear since a second protonation event would not disturb the $\pi$-system, but it is likely that the chain torsion effects described earlier prohibit doping of the material at high acid concentrations.

Two additional acids were investigated to examine the effects of different anions on the protonation and doping behavior of PBZT. Figure 9 shows the results for methane sulfonic acid ($CH_3SO_3H$, a common solvent for PBZT) and Figure 10 is for tetrafluorboric acid ($HBF_4$). At low acid concentrations (0 to 10.7 M, $pCH_3SO_3H > -1.0$

and 0 to 7.9 M, $pHBF_4 > -0.9$), the absorbance spectra are again similar to the previous two cases.  For both cases, as the acid concentration increases, the peaks at 443 nm and 474 nm decrease while the one at 499 grows, with an isosbestic point near 483 nm (Figures 9 and 10, a and b).  The inflection point of the spectrometric titration curve gives an estimated $pK_a$ for the first protonation event of $-0.9$ in $CH_3SO_3H$ and $-0.75$ in $HBF_4$. Additionally, at higher $CH_3SO_3H$ concentrations (Figure 9, c and d), the absorption curve again becomes blue-shifted, as seen for $H_2SO_4$, presumable due to the second protonation of PBZT causing an increase in the ring torsion angle, thereby shortening the conjugation length.  The estimated $pK_a$ for this second protonation event in $CH_3SO_3H$ is $-1.07$.  The sudden drop-off of the peak intensity at very high concentrations is due to the fact that the $CH_3SO_3H$ is beginning to dissolve PBZT.

Similar to the case for $H_2SO_4$, the PBZT film is able to be doped by Fe at intermediate $CH_3SO_3H$ concentrations.   This occurs between the first transition ($pK_a$ for mono-protonation, 7.6 M, $pCH_3SO_3H$ $-0.9$) and the second ($pK_a$ for the second protonation, 11.7 M, $pCH_3SO_3H$ $-1.07$).   At concentrations higher than this, the absorption spectrum undergoes a blue-shift and the film is unable to be doped by Fe.  In addition, Cu does not dope the film in $CH_3SO_3H$ at any concentration and neither Cu nor Fe will dope the film in $HBF_4$ at any concentration.

Examining the protonation and doping behavior of PBZT films in all four acids leads to some general trends.  Under all circumstances, the film must be in its mono-protonated state ($pHA < pK_a$ for mono-protonation) in order for it to be doped by simple metals (i.e. reduction potential significantly increased).   At higher acid concentrations, the film undergoes another transition, presumable the second protonation event, above which it

exhibits a blue shift in the absorbance spectrum and is unable to be doped by simple metals. This protonation behavior would appear to be independent of the acid used for the protonation (i.e. the shape of the absorption spectrum is about the same in all four cases). However, the doping behavior at intermediate acid concentrations can change significantly depending upon the anion that is present. In terms of reduction, the order from easiest to hardest is $Cl^- > (HSO_4^-, CH_3SO_3^-) > BF_4^-$ due to the fact that Cu will only dope PBZT in HCl, whereas Fe will dope the film in all but HBF$_4$. This trend can be considered based on the pK$_a$ values of each of these four acids and the relative basicities of the anions. Specifically, the pK$_a$ values and their relative order are HCl ($-7$) < H$_2$SO$_4$ ($-2$) < CH$_3$SO$_3$H ($-1.8$) < HBF$_4$ ($-0.44$)[63-65]. Despite the fact that these are all strong acids which will be completely dissociated in dilute aqueous solutions, there is still a good correlation with the ability of the PBZT to be reduced when protonated by these acids. It would seem that the basicity of the anion plays a significant role in determining the reduction potential of the protonated polymer with the least basic anion (i.e. the strongest acid, HCl) giving the largest values likely due to a smaller degree of interaction with the protonated chain.

**Conclusions**

A full description of the protonation and chemical doping behavior of thin films of PBZT was given. Protonation of the polymer backbone initially leads to a red-shift in the absorption spectrum. This was attributed to an electronic effect whereby the positive charge due to protonation of the N-lone pair electrons acted as an electron accepting substituent. The LUMO is lowered more so than the HOMO due to the greater electron

density on the N-site in the LUMO, thereby leading to a red-shift in the absorption spectrum. It was shown that when half of the N sites in the polymer backbone are protonated, the polymer is able to be easily reduced, even with simple metals, leading to relatively stable n-doped conducting polymers. These doped materials are stable with respect to water, however are slowly de-doped in an oxygen-containing environment due to re-oxidation. Generically, this effect occurs independent of the acid used, however the nature of the counter-anion does play a smaller role in determining the exact value of the reduction potential. At higher acid concentrations the absorption spectrum exhibits a blue-shift, due to the polymer becoming fully protonated, and this doping effect is not observed. This is attributed to a decrease in the intermolecular chain interactions leading to a loss of coplanarity between the heterocyclic and phenyl rings in the polymer. This results in a lowering of the effective conjugation length and a smaller degree of electron delocalization along the backbone.
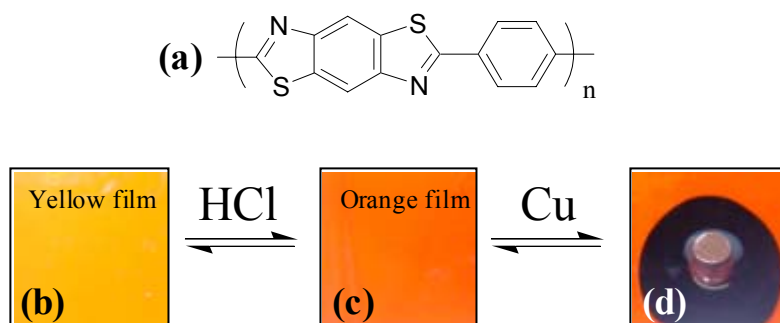
**Acknowledgements**

Figure 1 – Chemical structure of poly(benzobisthiozole) (PBZT) (a), and images of an extruded film of PBZT immersed in water (b), concentrated (37 weight %) hydrochloric acid (c), and concentrated hydrochloric acid while in contact with Cu (d).
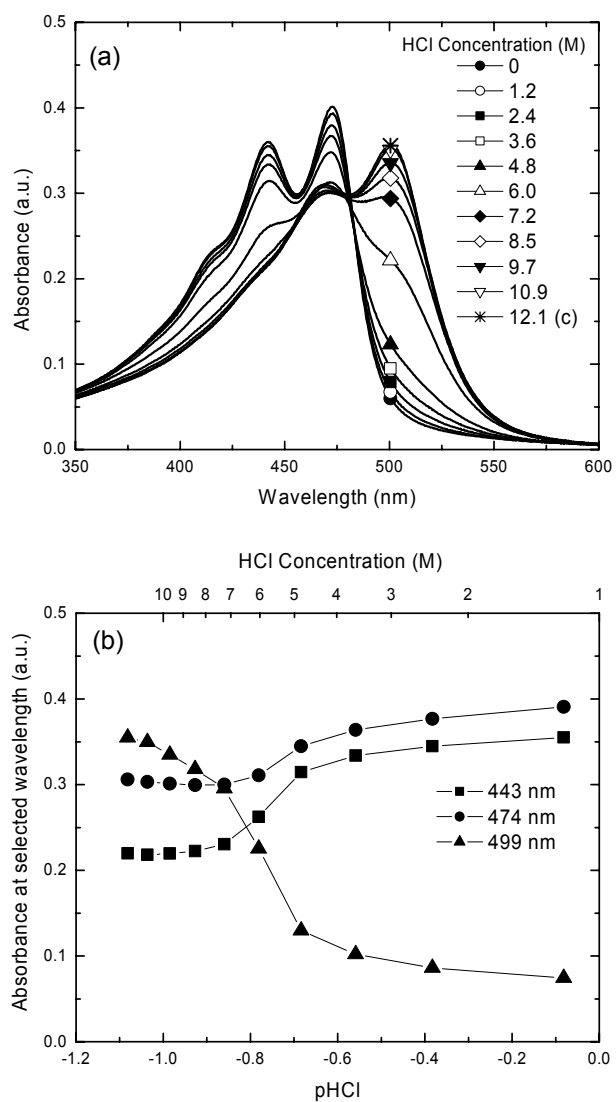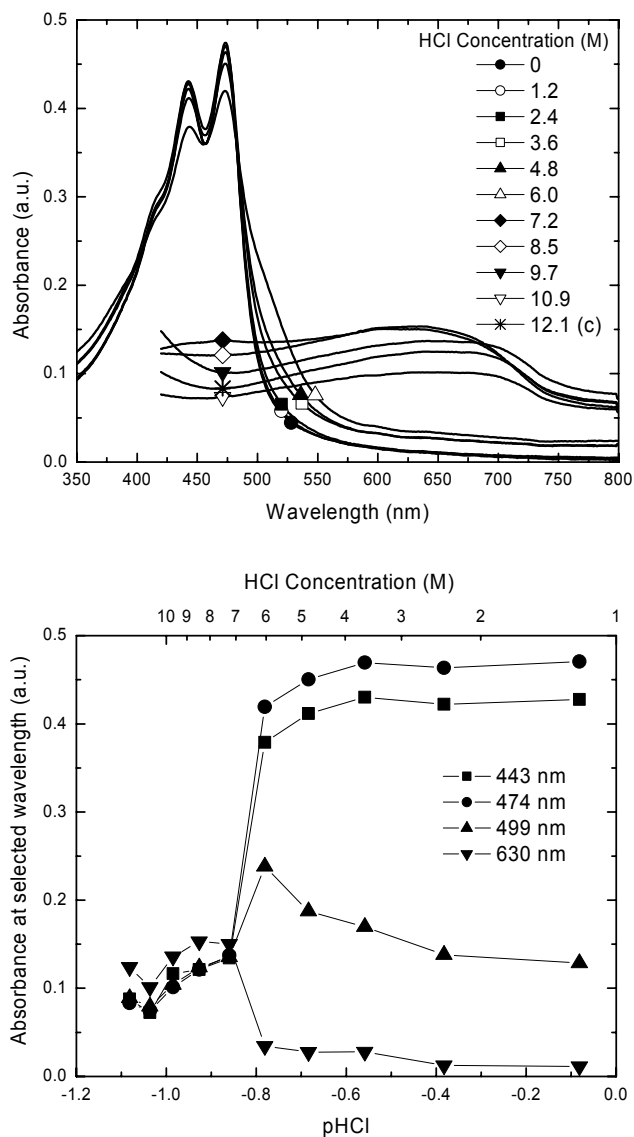
Figure 2 - Absorbance spectra of PBZT thin films immersed in aqueous solutions of hydrochloric acid at various concentrations (a), and peak intensities of the absorbance spectra at selected wavelengths as a function of pHCl = -log[HCl] (b).

Figure 3 - Absorbance spectra of PBZT thin films in contact with copper metal and immersed in aqueous solutions of hydrochloric acid at various concentrations (a), and peak intensities of the absorbance spectra at selected wavelengths as a function of pHCl = -log[HCl] (b).
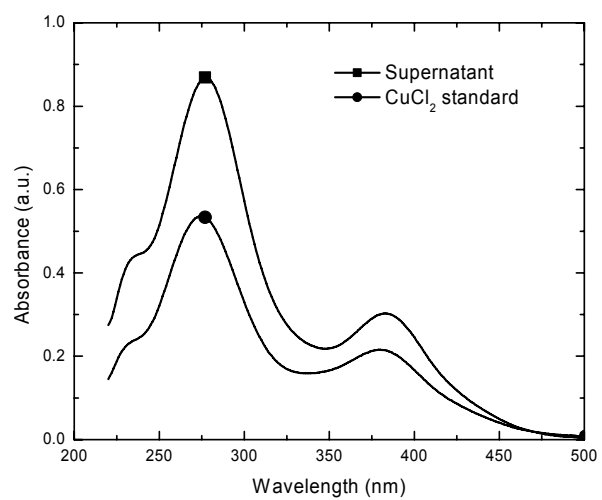
Figure 4 - UV-visible absorption spectra of supernatant solution after doping PBZT film with Cu, and control solution of $CuCl_2$ in concentrated hydrochloric acid.
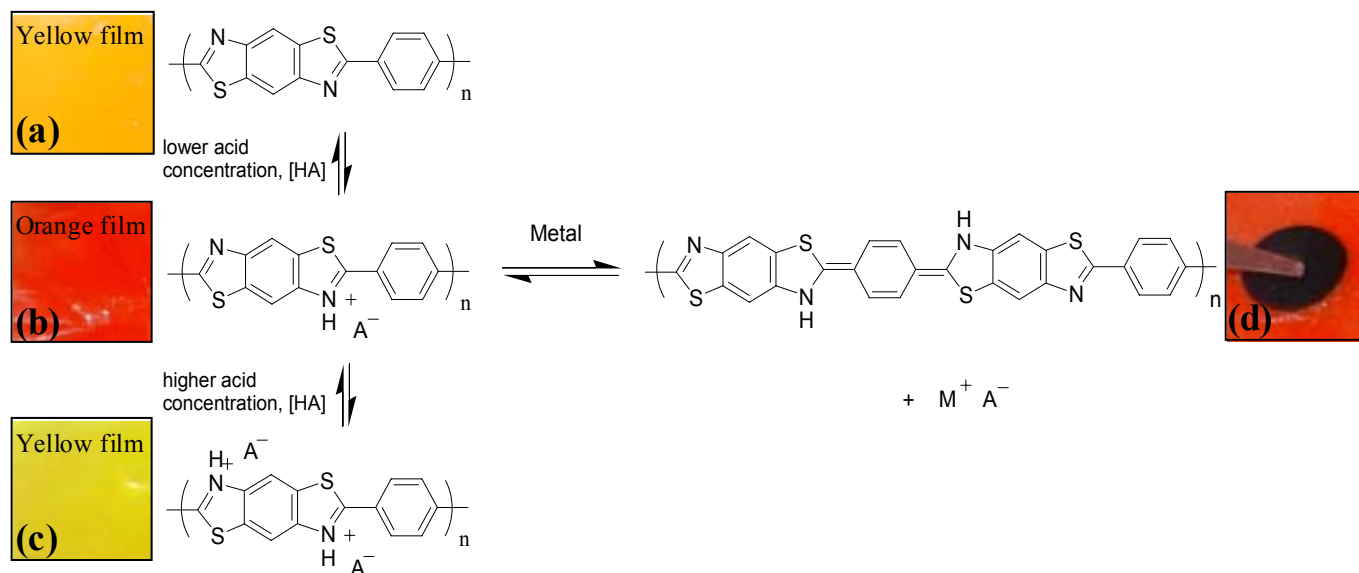
Figure 5 – Protonation and chemical doping behavior of an extruded film of PBZT immersed in water (a), a lower acid concentration (b), a higher acid concentration (c), and a lower acid concentration while in contact with a simple metal (d). The structures are drawn for the generic case of different acids and metals, while the images were taken for the specific case of $H_2SO_4$ (53 wt% and 96 wt% for the lower and higher concentrations, respectively) and Fe metal.
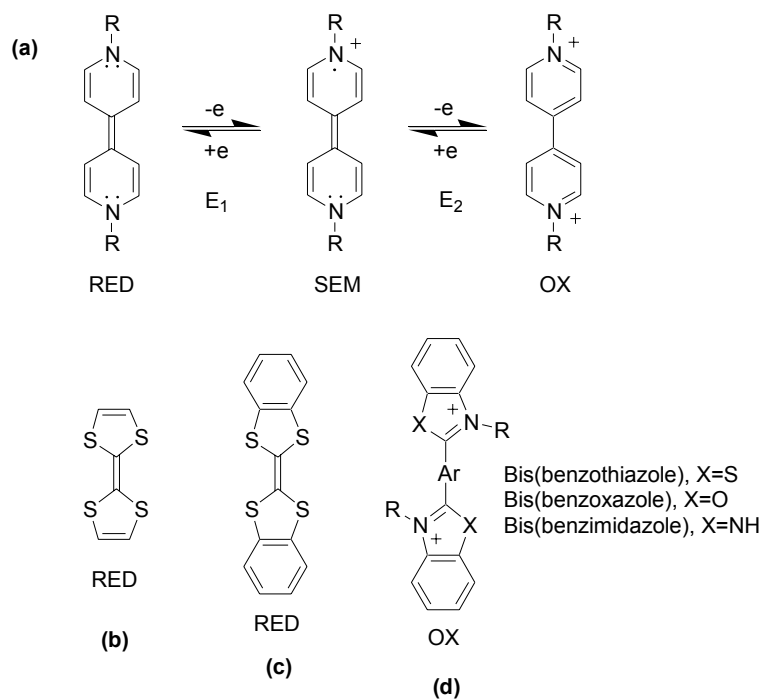
Figure 6 – The viologen system illustrating the reduced, semiquinone, and oxidized redox states (a), and a series of related compounds which also exhibit Weitz-type behavior: tetrathiafulvalene (b), dibenzo-tetrathiafulvalene (c), and a series of benzazoles (d).
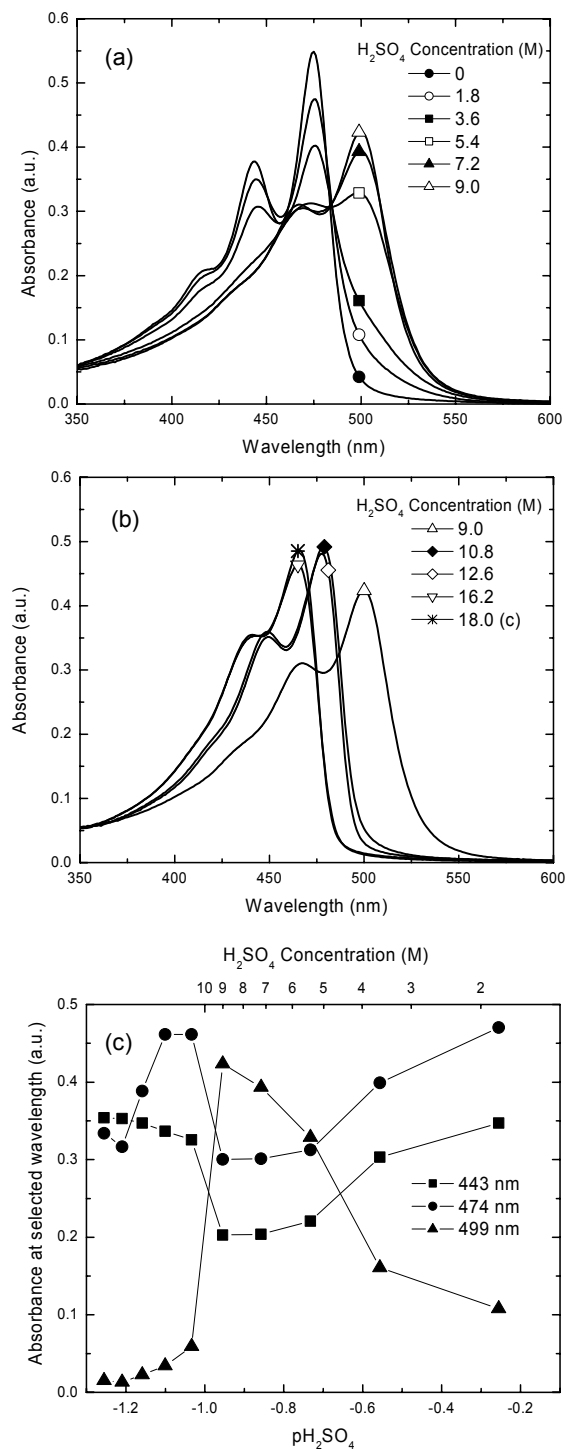
Figure 7 - Absorbance spectra of PBZT thin films immersed in aqueous solutions of sulfuric acid at various concentrations (a) and (b), and peak intensities of the absorbance spectra at selected wavelengths as a function of $pH_2SO_4$ = -log[$H_2SO_4$] (c).
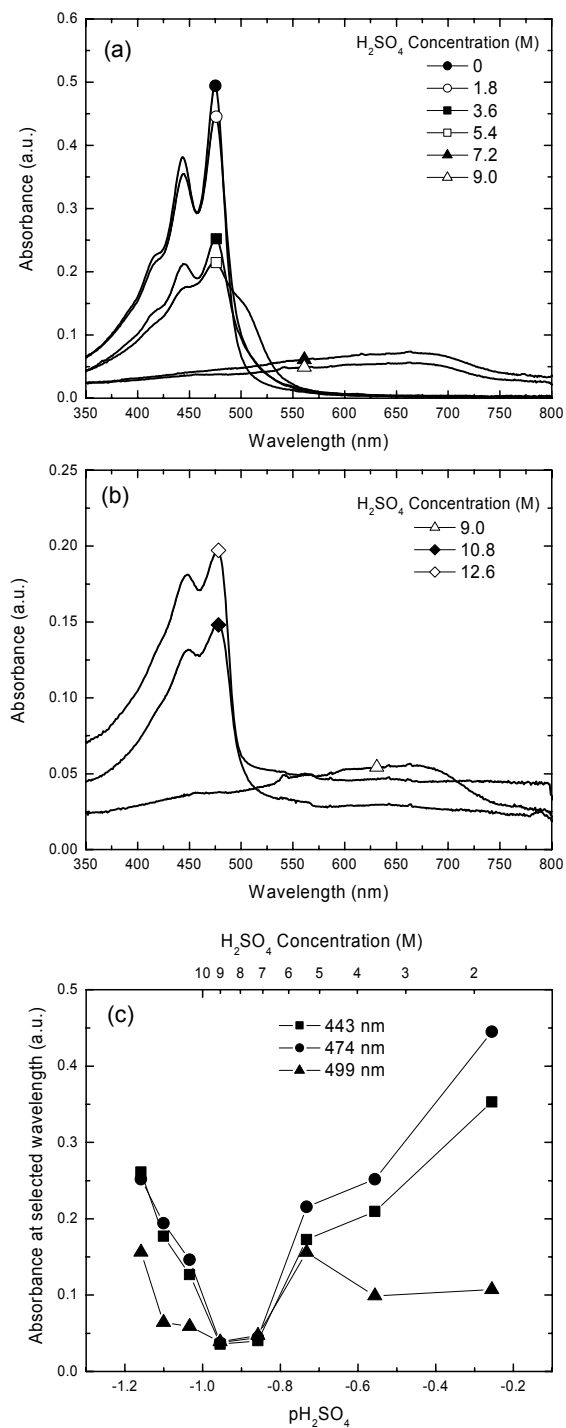
Figure 8 - Absorbance spectra of PBZT thin films in contact with iron metal and immersed in aqueous solutions of sulfuric acid at various concentrations (a) and (b), and peak intensities of the absorbance spectra at selected wavelengths as a function of $pH_2SO_4 = -\log[H_2SO_4]$ (c).
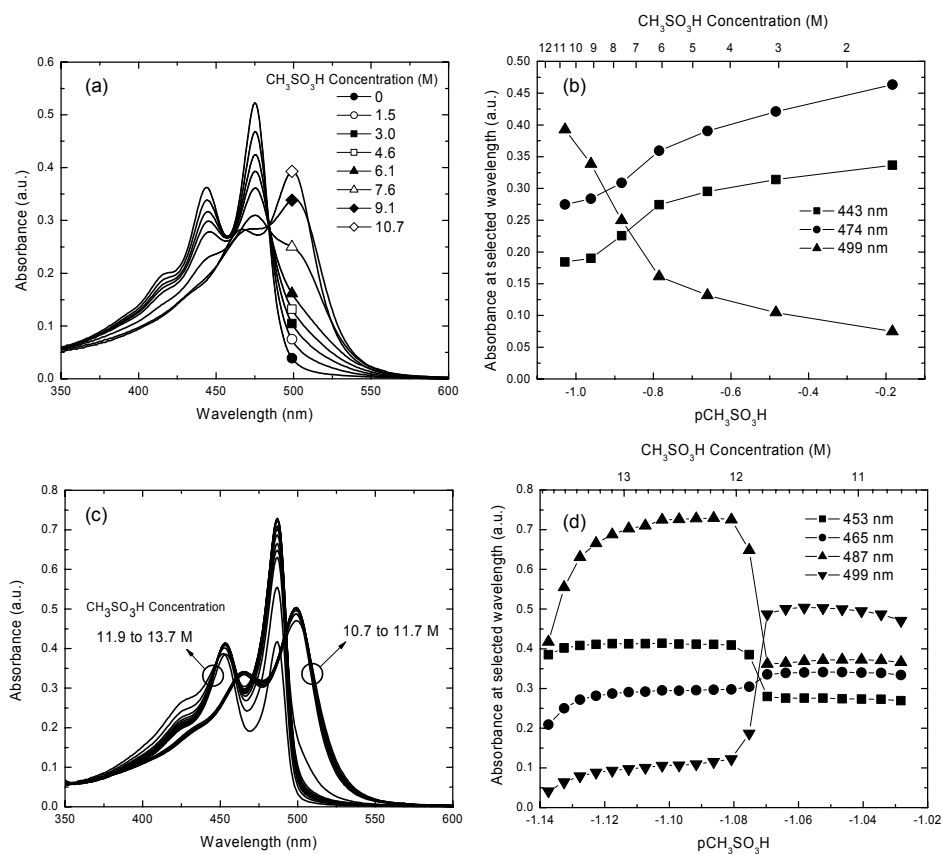
Figure 9 - Absorbance spectra of PBZT thin films immersed in aqueous solutions of methane sulfonic acid at various concentrations (a) and (c), and peak intensities of the absorbance spectra at selected wavelengths as a function of $pCH_3SO_3H = -log[CH_3SO_3H]$ (b) and (d).
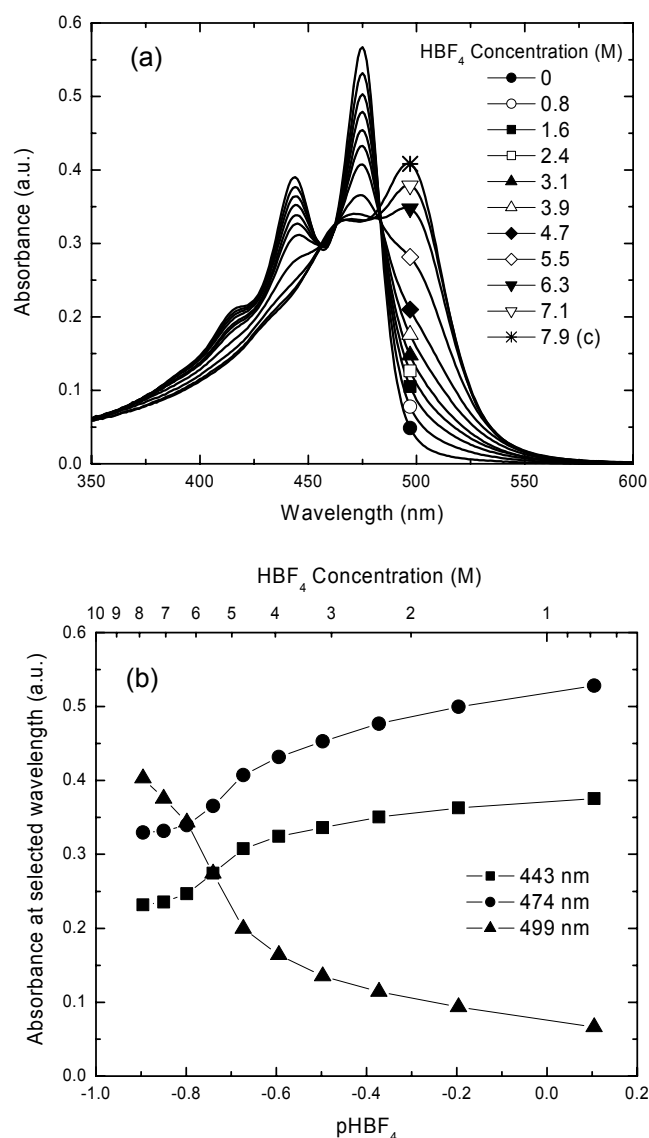
Figure 10 - Absorbance spectra of PBZT thin films immersed in aqueous solutions of tetrafluoroboric acid at various concentrations (a), and peak intensities of the absorbance spectra at selected wavelengths as a function of $pHBF_4$ = -log[$HBF_4$]  (b).

(1)     Yamamoto, T.;  Maruyama, T.;  Zhou, Z.-h.;  Ito, T.;  Fukuda, T.;  Yoneda, Y.;  Begum, F.;  Ikeda, T.;  Sasaki, S.;  Takezoe, H.;  Fukuda, A.; Kubota, K. *J. Am. Chem. Soc.* **1994**, *116*, 4832-4845.

(2)     Jenkins, I. H.;  Rees, N. G.; Pickup, P. G. *Chem. Mater.* **1997**, *9*, 1213-1216.

(3)     deLeeuw, D. M.; Simenon, M. M. J.; Brown, A. R.; Einerhand, R. E. F. *Synth. Met.* **1997**, *87*, 53-59.

(4)     Arbizzani, C.; Catellani, M.; Mastragostino, M.; Mingazzini, C. *Electrochim. Acta* **1995**, *40*, 1871-1876.

(5)     Curtis, M. D.; Cheng, H.; Johnson, J. A.; Nanos, J. I. *Chem. Mater.* **1998**, *10*, 13-16.

(6)     Politis, J. K.; Curtis, M. D.; He, Y.; Kanicki, J. *Macromolecules* **1999**, *32*, 2484-2489.

(7)     Alexander, M. A.; Vaia, R. A.; Dudis, D. S.; Wang, C.-S.; Lee, J.-W.; Centennial Meeting, American Physical Society, Atlanta GA (March 1999), 1999.

(8)     Alexander, M. D.; Dudis, D. S.; McKellar, B. R. *Polymer Preprints* **2000**, *41*, 358.

(9)     McClain, M. D.; Dudis, D. S. *Polymer Preprints* **2000**, *41*, 233.

(10)    Dudis, D. S.; McKellar, B. R. *Polymer Preprints* **2000**, *41*, 235.

(11)    McKellar, B. R.; Dudis, D. S.; Sankaran, B.; Alexander, M. D.; Tan, L.-S. *Polymer Preprints* **2000**, *41*, 242.

(12)    Alexander, M. D.; Specker, C. E.; Dudis, D. S.; McKellar, B. R. In *197th meeting of the Electrochemical Society*, 2000; Vol. 2000-I, p Abstract No. 1072.

(13)    Alexander, M. D.; Sankaran, B.; McKellar, B. R.; Dudis, D. S. In *Materials Research Society*, 2001; Vol. 665, pp C8.35.31-36.

(14)    McClain, M. D.; Dudis, D. S. *Synth. Met.* **2001**, *116*, 199-202.

(15)    Facchetti, A.; Deng, Y.; Wang, A.; Koide, Y.; Sirringhaus, H.; Marks, T. J.; Friend, R. H. *Angewandte Chemie International Edition* **2000**, *39*, 4547.

(16)    Facchetti, A.; Yoon, M.-H.; Katz, H. E.; Marks, T. J., Eds. *Materials for n-type organic electronics. Synthesis and properties of fluoroarene-thiophene semiconductors*, 2003.

(17)    Facchetti, A.; Yoon, M.-H.; Stern, C. L.; Katz, H. E.; Marks, T. J. *Angewandte Chemie International Edition* **2003**, *42*, 3900-3903.

(18)    Facchetti, A.; Mushrush, M.; Katz, H.; Marks, T. *Adv. Mater.* **2003**, *15*, 33-38.

(19)    Facchetti, A.; Yoon, M.-H.; Stern, C. L.; Hutchison, G. R.; Ratner, M. A.; Marks, T. J. *J. Am. Chem. Soc.* **2004**, *126*, 13480-13501.

(20)    Facchetti, A.; Mushrush, M.; Yoon, M.-H.; Hutchison, G. R.; Ratner, M. A.; Marks, T. J. *J. Am. Chem. Soc.* **2004**, *126*, 13859-13874.

(21)    Yoo, B.; Jung, T.; Basu, D.; Dodabalapur, A.; Jones, B. A.; Facchetti, A.; Wasielewski, M. R.; Marks, T. J. *Applied Physics Letters* **2006**, *88*, 082104.

(22)    Yoon, M.-H.; DiBenedetto, S. A.; Facchetti, A.; Marks, T. J. *J. Am. Chem. Soc.* **2005**, *127*, 1348-1349.

(23)    Bao, Z.; Lovinger, A. J.; Brown, J. *J. Am. Chem. Soc.* **1998**, *120*, 207-208.

(24)    Brown, A. R.; Leeuw, D. M. d.; Lous, E. J.; Havinga, E. E. *Synth. Met.* **1994**, *66*, 257-261.

(25)    Chesterfield, R. J.; Newman, C. R.; Pappenfus, T. M.; Ewbank, P. C.; Haukaas, M. H.; Mann, K. R.; Miller, L. L.; Frisbie, C. D. *Adv. Mater.* **2003**, *15*, 1278.

(26)    Crone, B.; Dodabalapur, A.; Lin, Y.-Y.; Filas, R. W.; Bao, Z.; LaDuca, A.; Sarpeshkar, R.; Katz, H. E.; Li, W. *Nature* **2000**, *403*, 521.

(27)    Heidenhain, S. B.; Sakamoto, Y.; Suzuki, T.; Miura, A.; Fujikawa, H.; Mori, T.; Tokito, S.; Taga, Y. *J. Am. Chem. Soc.* **2000**, *122*, 10240-10241.

(28)    Katz, H. E.; Johnson, J.; Lovinger, A. J.; Li, W. *J. Am. Chem. Soc.* **2000**, *122*, 7787-7792.

(29)    Katz, H. E.; Lovinger, A. J.; Johnson, J.; Kloc, C.; Siegrist, T.; Li, W.; Lin, Y.-Y.; Dodabalapur, A. *Nature* **2000**, *404*, 478.

(30)    Laquindanum, J. G.; Katz, H. E.; Dodabalapur, A.; Lovinger, A. J. *J. Am. Chem. Soc.* **1996**, *118*, 11331.

(31)    Malenfant, P. R. L.; Dimitrakopoulos, C. D.; Gelorme, J. D.; Kosbar, L. L.; Graham, T. O.; Curioni, A.; Andreoni, W. *Applied Physics Letters* **2002**, *80*, 2517.

(32)    Pappenfus, T. M.; Chesterfield, R. J.; Frisbie, C. D.; Mann, K. R.; Casado, J.; Raff, J. D.; Miller, L. L. *J. Am. Chem. Soc.* **2002**, *124*, 4184.

(33)    Renak, M. L.; Bartholomew, G. P.; Wang, S.; Ricatto, P. J.; Lachicotte, R. J.; Bazan, G. C. *J. Am. Chem. Soc.* **1999**, *121*, 7787-7799.

(34)    Yassar, A.; Demanze, F.; Jaafari, A.; Idrissi, M. E.; Coupry, C. *Advanced Functional Materials* **2002**, *12*, 699.

(35)    Adams, W. W.; Eby, R. K.; McLemore, D. E., Eds. *Materials Research Society Symposium Proceedings*, 1988; Vol. 134.

(36)    Decher, G. *Science* **1997**, *277*, 1232.

(37)    Durstock, M. F.; Rubner, M. F. *Langmuir* **2001**, *17*, 7865-7872.

(38)    Yoo, D.; Shiratori, S. S.; Rubner, M. F. *Macromolecules* **1998**, *31*, 4309-4318.

(39)    Shiratori, S. S.; Rubner, M. F. *Macromolecules* **2000**, *33*, 4213-4219.

(40)    DePra, P. A.; Gaudiello, J. G.; Marks, T. J. *Macromolecules* **1988**, *21*, 2295-2297.

(41)    Shen, D. Y.; Venkatesh, G. M.; Burchell, D. J.; Shu, P. H. C.; Hsu, S. L. *Journal of Polymer Science: Polymer Physics Edition* **1982**, *20*, 509-521.

(42)    Venkatesh, G. M.; Shen, D. Y.; Hsu, S. L. *Journal of Polymer Science: Polymer Physics Edition* **1981**, *19*, 1475-1488.

(43)    Jenekhe, S. A.; Paor, L. R. d.; Chen, X. L.; Tarkka, R. M. *Chem. Mater.* **1996**, *8*, 2401-2404.

(44)    Pan, J.-F.; Chen, Z.-K.; Chua, S.-J.; Huang, W. *J. Phys. Chem. A* **2001**, *105*, 8775-8781.

(45)    Eichen, Y.; Nakhmanovich, G.; Gorelik, V.; Epshtein, O.; Poplawski, J. M.; Ehrenfreund, E. *J. Am. Chem. Soc.* **1998**, *120*, 10463-10470.

(46)    Monkman, A. P.; Halim, M.; Samuel, I. D. W.; Horsburgh, L. E. *J. Chem. Phys.* **1998**, *109*, 10372-10378.

(47)    Polster, J.; Lachmann, H. *Spectrometric Titrations: Analysis of Chemical Equilibria*; VCH Publishers: New York, 1989.

(48)    Kaim, W. *Angew. Chem. Int. Ed. Engl.* **1983**, *22*, 171-189.

(49)    Moissette, A.; Batonneau, Y.; Bremard, C. *J. Am. Chem. Soc.* **2001**, *123*, 12325-12334.

(50)    Bard, A. J. *Chemical Equilibrium*; Harper & Row, Publishers: New York, 1966.

(51)    Hunig, S.; Berneth, H. In *Topics in Current Chemistry*; Boschke, F. L., Ed., 1980; Vol. 92, pp 1-44.

(52)    Weitz, E. *Angew. Chem.* **1954**, *66*, 658.

(53)    Weitz, E.; Fischer, K. *Angew. Chem.* **1925**, *38*, 1110.

(54)    Deuchert, K.; Hunig, S. *Angew. Chem. Int. Ed. Engl.* **1978**, *17*, 875-886.

(55)    Hunig, S. *Pure & Appl. Chem.* **1990**, *62*, 395-406.

(56)    Bryce, M. R.; Fleckenstein, E.; Hunig, S. *J. Chem. Soc. Perkin Trans. 2* **1990**, *11*, 1777-1783.

(57)    Wellman, M. W.; Adams, W. W.; Wolff, R. A.; Dudis, D. S.; Wiff, D. R.; Fratini, A. V. *Macromolecules* **1981**, *14*, 935-939.

(58)    Welsh, W. J.; Bhaumik, D.; Mark, J. E. *Macromolecules* **1981**, *14*, 947-950.

(59)    Bhaumik, D.; Welsh, W. J.; Jaffe, H. H.; Mark, J. E. *Macromolecules* **1981**, *14*, 951-953.

(60)    Fratini, A. V.; Lenhert, P. G.; Resch, T. J.; Adams, W. W. In *Materials Research Society*, 1988; Vol. 134, pp 431-446.

(61)    Farmer, B. L.; Wierschke, S. G.; Adams, W. W. In *Materials Research Society*, 1988; Vol. 134, pp 447-455.

(62)    Welsh, W. J.; Mark, J. E.; Yang, Y.; Das, G. P. In *Materials Research Society*, 1988; Vol. 134, pp 621-633.

(63)    Oxtoby, D. W.; Nachtrieb, N. H. *Principles of Modern Chemistry*; CBS College Publishing, 1986.

(64)    McMurry, J. *Organic Chemistry*; Brooks/Cole Publishing Company: Belmont, California, 1992.

(65)    MacFarlane, D. R.; Pringle, J. M.; Johansson, K. M.; Forsyth, S. A.; Forsyth, M. *Chem. Commun.* **2006**, 1905-1917.